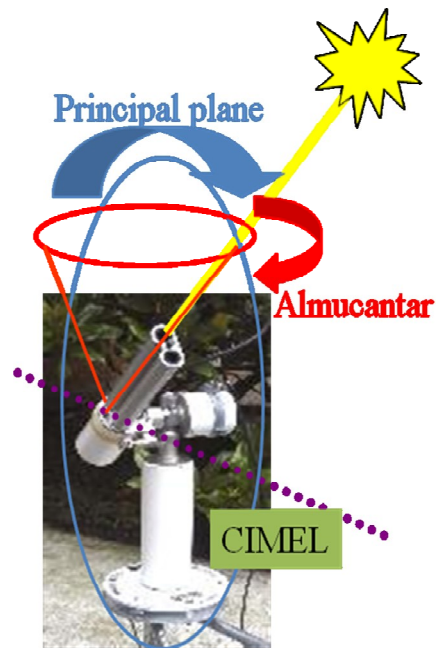


Lecture 10. Ground-based measurements Cont'd

1. CIMEL Sunphotometer

$$\frac{I}{I_0} = \exp(-\varepsilon_{ext} z) = \exp(-\tau)$$

CIMEL sunphotometer (http://www.cimel.fr/photo/sunph_us.htm) operates automatically without operator assistance. It measures direct solar irradiance by first pointing the collimator toward the approximate position of the sun (provided it is aligned properly) based on an in-built program that takes into account the time of the year and the coordinates of the location that are input to the CIMEL control box prior to operation. A 4-quadrant detector then positions the sun at the center of the fields of view of the collimators by using a feedback control loop. The filter wheel rotates in front of the detector to obtain a measurement sequence. A sequence takes about 10 seconds. In order to discriminate against the presence of thin cirrus clouds, which may be non-uniform, three measurement sequences are performed (called as a triplet), lasting about 35 seconds. During a data analysis procedure, the measured voltages are compared to eliminate non-uniform scenes. **Almucantar** sky radiance is obtained by scanning the sky at the solar zenith angle but different azimuth angles to obtain the angular variation of skylight in 4 filters. **Solar principal plane** sky measurement is obtained by scanning the sky in a plane containing the sun and the instrument and normal to the surface. Data are taken more frequently near the sun since the intensity varies rapidly in the solar aureole. The sky brightness data is inverted by radiative transfer routines to derive aerosol size distribution and phase function.



Theory of Operations. The direct normal solar irradiance I [w/m^2] at the surface at a given wavelength is given by Bouguer's law:

$$I_h = \frac{I_0}{r^2} \exp(-\tau m)$$

where I_0 is the mean solar irradiance at top of the atmosphere, r is the ratio of the earth-sun distance to its mean value, m is the airmass and τ is the total vertical optical thickness. The total optical thickness is made up of molecular

(Rayleigh), trace gas (e.g. O₃) and aerosol attenuations. By appropriately estimating the molecular and ozone contributions, aerosol optical thickness can be estimated from the measured voltage V for irradiance I :

$V = \frac{V_0}{r^2} \exp(-\tau m)$ where V_0 is the calibration coefficient obtained by measuring V as a function of airmass m and extrapolating the resulting curve to zero airmass. The accuracy in the estimation depends on the uncertainty in V and uncertainty in V_0 .

The former is a function of the precision of the silicon detector which is very high and therefore ratio between the actual to the average can be neglected. Accuracy in the calibration coefficient is 0.2 to 0.5% for the reference instrument. Therefore the uncertainty in AOT due to the uncertainty in zero airmass voltages for the reference instruments is better than 0.002 to 0.005. The other instruments are intercalibrated against the reference instrument both before deployment in the field and post- deployment. A linear rate of change in time of the zero airmass voltages is then assumed in the processing of the data from field sites. The accuracy of field instruments is about 0.01-0.02 in aerosol optical thickness due to calibration uncertainty for the field instrument.

AERONET. A global network of sunphotometers CIMEL instruments are federated through the NASA Goddard Aerosol RObotic NETwork (AERONET) program (<http://aeronet.gsfc.nasa.gov>). AERONET data provide globally distributed observations of spectral aerosol optical depth (AOD), inversion products, and precipitable water in diverse aerosol regimes. Aerosol optical depth data are computed for three data quality levels: Level 1.0 (unscreened), Level 1.5 (cloud screened), and Level 2.0 (cloud-screened and quality-assured). Inversions, precipitable water, and other AOD-dependent products are derived from these levels and may implement additional quality checks.



AERONET DATA	
Data Format	Description
All Points	These data are available for each measurement or retrieval moment.

Daily Average	These data are calculated from all points for each day when three (3) or more points are available.
Monthly Average of Daily Averages	These data are calculated using the daily average for each day to compute the monthly average. $\bar{X} = \frac{\sum X_i}{n}$
Monthly Average of Weighted Daily Averages	These data are calculated using the weighted daily average for each day to compute the monthly average. $\bar{X} = \frac{\sum (X_i n_i)}{\sum n_i}$

Data Type	Description
Aerosol Optical Thickness (AOT)	
Level 1.0 (Raw)	Unscreened and may not have final calibration applied
Level 1.5 (Cloud Screened)	Automatically cloud cleared but may not have final calibration applied. These data are NOT quality assured.
Level 2.0 (Quality Assured)	Pre- and post-field calibration, automatically cloud cleared and manually inspected
Precipitable Water	The total water vapor in the column derived from the 935nm channel.
Percent Triplet Variability	Each AOT measurement is comprised of a triplet measurement: These measurements are taken every 30 seconds for one minute. The variability of this measurement can provide insight on the quality of the data.
Angstrom Parameter	The angstrom parameter is calculated for every instance of each AOT data level. The angstrom (670-440) includes the 670, 500 and 440 nm AOT data. A special case is angstrom (670-440 polar) which only includes 670 and 440 nm AOT data (500 nm is not measured).
Dubovik Almucantar Retrievals	
Size Distribution	Derived aerosol size distribution
Refractive Index	Derived refractive index of the atmosphere (real and imaginary parts)
SSA	Derived single scattering albedo (total, fine and coarse modes)
AOT Coincident	Calculated by averaging the level 1.5 or 2.0 AOT data values (Level 2.0 has priority) +/- 16 minutes of the almucantar retrieval time (typically uses three to five AOT points for the

Volume	Volume concentration, volume median radius, effective radius, standard deviation (total, fine and coarse modes)
AOT Extinction	Derived values for AOT from almucantar retrieval (total, fine and coarse modes). The total mode is determined by the sum of the fine and coarse modes.
Asymmetry Factor	Integrated value for phase functions (total, fine and coarse modes)
Phase Functions	Calculated phase functions (total, fine and coarse modes)
Combined Retrievals	Combination of all Dubovik Almucantar Retrievals except phase functions.
AOT Absorption	Equation: $(1-SSA)*AOT$ (where AOT is AOT Extinction)- The single scattering albedo is used for each incidence of an almucantar retrieval. The AOT is calculated by adding the derived almucantar AOT fine and coarse modes. AOT absorption is calculated for the following channels:

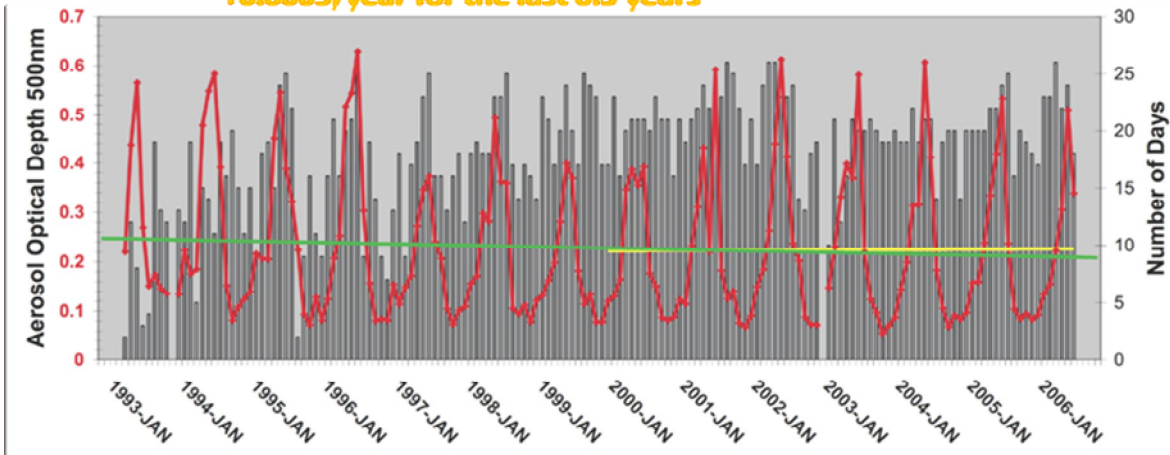
Analysis of AERONET data

In 1993 only 25 instruments were operating, while now more than 200 are operating. of AOD. With almost 15 years of data, trends can be determined.

AOD(550nm) Trends in Greenbelt, MD

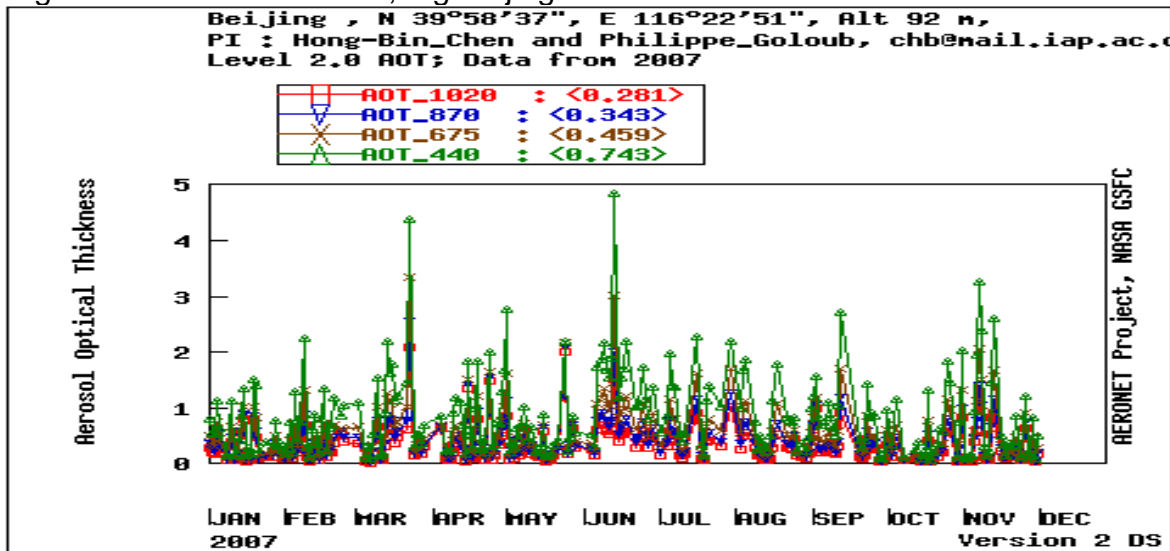
-0.002/year for the last 13 years

+0.0005/year for the last 6.5 years

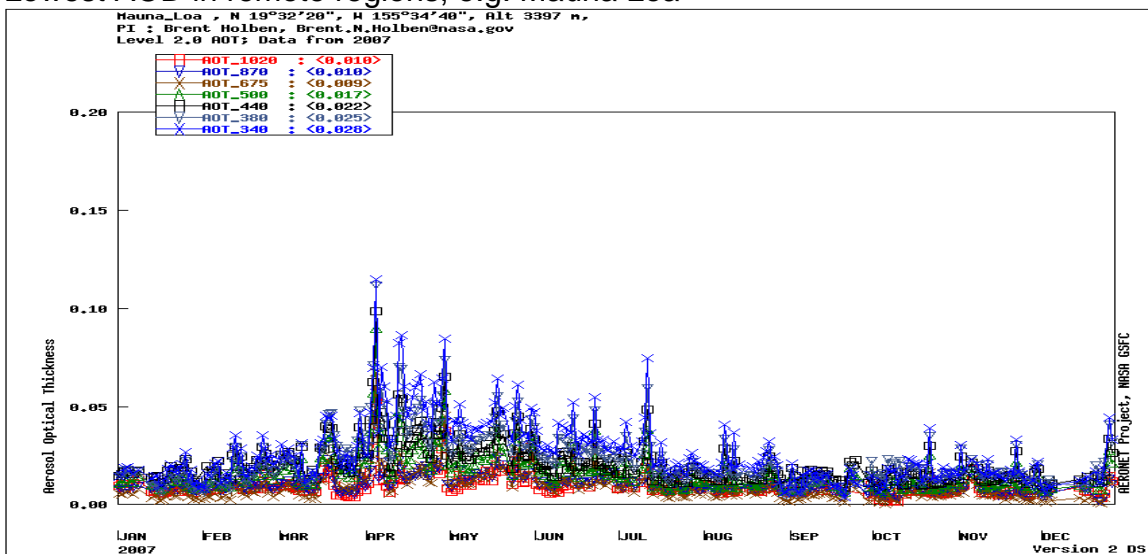


The estimated global mean value of AOD at 550 nm from all sites is about 0.17. With a background value of about 0.05 (550nm) covering most of the open oceans, it indicates the important loading of aerosols in the polluted regions and desert area, most in the northern hemisphere.

Highest AOD in urban area, e.g. Beijing



Lowest AOD in remote regions, e.g. Mauna Loa

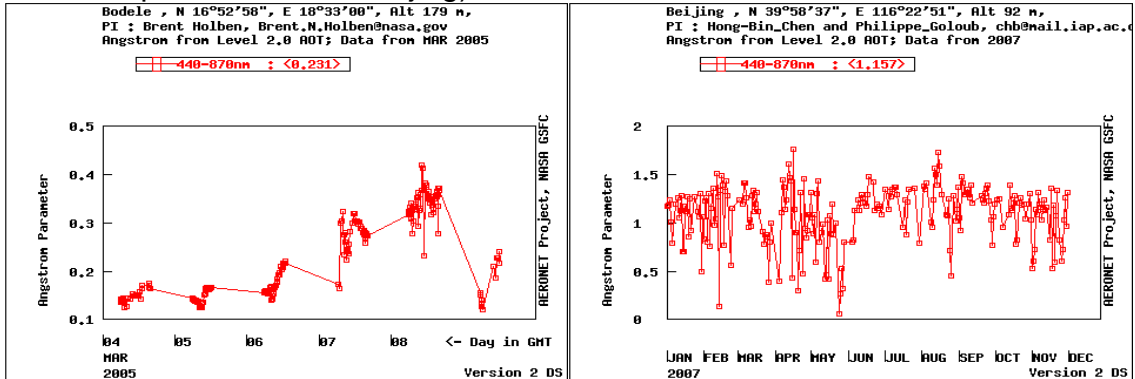


Angstrom exponent

The Angstrom exponent α defined by the spectral dependence (on wavelength λ) of optical thickness $\tau(\lambda) \approx \lambda^{-\alpha}$. It is calculated from the measurement of τ at 2

wavelengths (λ_1, λ_2) and is given by $\alpha = -\frac{\ln \frac{\tau_1}{\tau_2}}{\ln \frac{\lambda_1}{\lambda_2}}$. The values of α are sensitive to

the size of the particles with lower values for coarse particles (less than 0.5 for dust as in Bodele depression), and higher values for fine particles (greater than 1 for urban pollutants as in Beijing)



Retrieved aerosol properties

The almucantar sky-radiance measurements are inverted to retrieve optical properties such as refractive index, volume size distribution, phase function,...

These properties are used to characterize aerosol optical properties for different environments

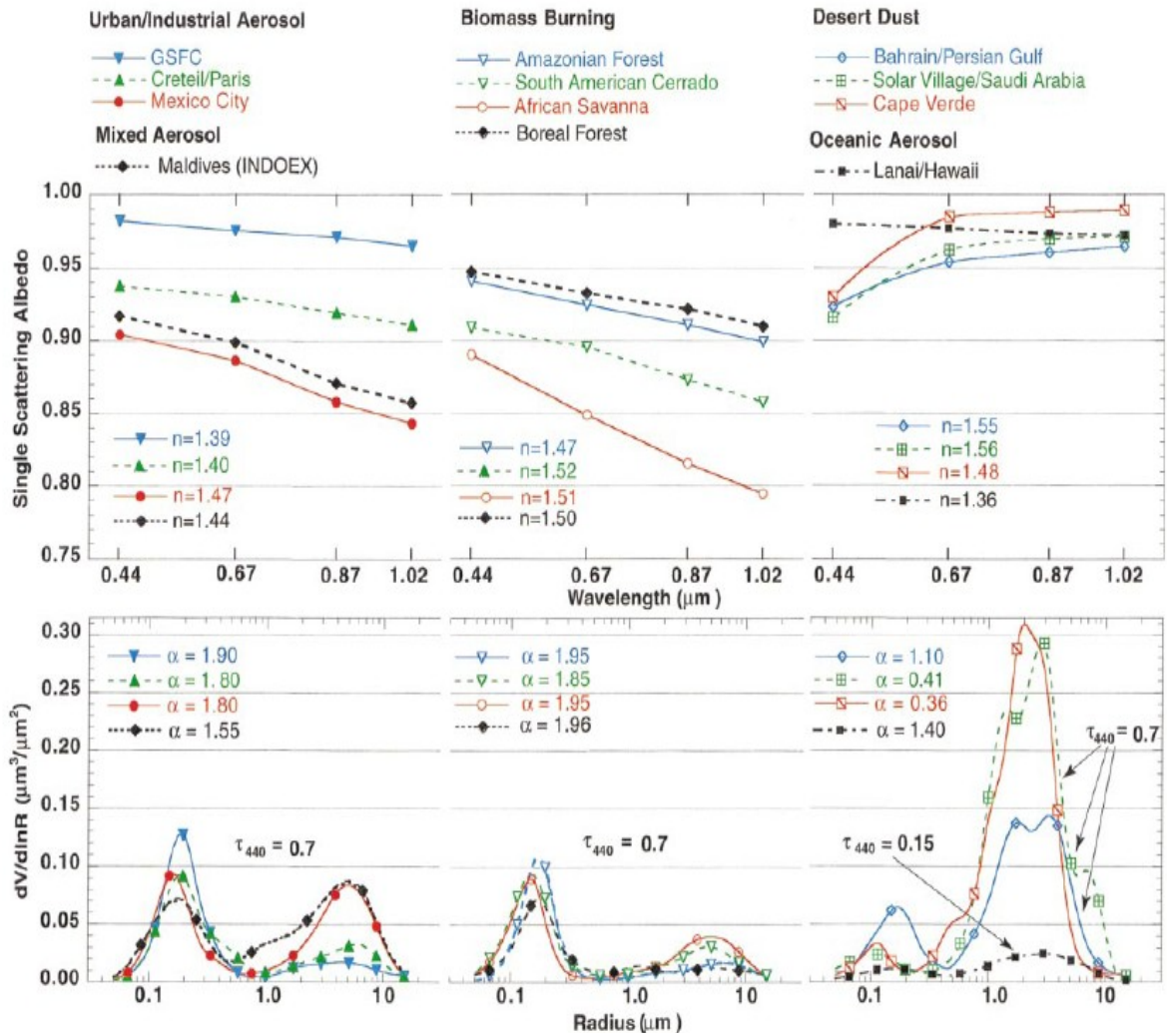


Figure 1 Aerosol optical properties retrieved from Almucentar sky-radiance data by Dubovik et al. (2002)

Table 1 Summary of aerosol optical properties retrieved from almucantar sky-radiance data by Dubovik et al. (2002)

Urban-industrial and mixed	GSFC, Greenbelt, MD (1993–2000)	Crete–Paris, France (1999)
Number of measurements (total)	2400	300
Number of measurements (for ω_0, n, k)	200 (Jun–Sep)	40 (Jun–Sep)
Range of optical thickness; $\langle\tau\rangle$	$0.1 \leq \tau(440) \leq 1.0$; $\langle\tau(440)\rangle = 0.24$	$0.1 \leq \tau(440) \leq 0.9$; $\langle\tau(440)\rangle = 0.26$
Range of Ångström parameter (g) (440/670/870/1020)	$1.2 \leq \alpha \leq 2.5$	$1.2 \leq \alpha \leq 2.3$
$n; k$	$0.68/0.59/0.54/0.53 \pm 0.08$	$0.68/0.61/0.58/0.57 \pm 0.07$
$\omega_0(440/670/870/1020)$	$1.41 - 0.03\tau(440) \pm 0.01$; 0.003 ± 0.003	1.40 ± 0.03 ; 0.009 ± 0.004
$r_{VF} (\mu\text{m}); \sigma_r$	$0.98/0.97/0.96/0.95 \pm 0.02$	$0.94/0.93/0.92/0.91 \pm 0.03$
$r_{Vs} (\mu\text{m}); \sigma_s$	$0.12 + 0.11 \tau(440) \pm 0.03$; 0.38 ± 0.01	$0.11 + 0.13 \tau(440) \pm 0.03$; 0.43 ± 0.05
$C_{VF} (\mu\text{m}^3/\mu\text{m}^2)$	$3.03 + 0.49 \tau(440) \pm 0.21$; 0.75 ± 0.03	$2.76 + 0.48 \tau(440) \pm 0.30$; 0.79 ± 0.05
$C_{Vs} (\mu\text{m}^3/\mu\text{m}^2)$	$0.15 \tau(440) \pm 0.03$	$0.01 + 0.12 \tau(440) \pm 0.04$
	$0.01 + 0.04 \tau(440) \pm 0.01$	$0.01 + 0.05 \tau(440) \pm 0.02$
	Amazonian forest, Brazil (1993–1994); Bolivia (1998–1999)	South American cerrado, Brazil (1993–1995)
Biomass burning		
Number of measurements (total)	700	550
Number of measurements (for ω_0, n, k)	250 (Aug–Oct)	350 (Aug–Oct)
Range of optical thickness; $\langle\tau\rangle$	$0.1 \leq \tau(440) \leq 3.0$; $\langle\tau(440)\rangle = 0.74$	$0.1 \leq \tau(440) \leq 2.1$; $\langle\tau(440)\rangle = 0.80$
Range of Ångström parameter (g) (440/670/870/1020)	$1.2 \leq \alpha \leq 2.1$	$1.2 \leq \alpha \leq 2.1$
$n; k$	$0.69/0.58/0.51/0.48 \pm 0.06$	$0.67/0.59/0.55/0.53 \pm 0.03$
$\omega_0(440/670/870/1020)$	1.47 ± 0.03 ; 0.00093 ± 0.003	1.52 ± 0.01 ; 0.015 ± 0.004
$r_{VF} (\mu\text{m}); \sigma_r$	$0.94/0.93/0.91/0.90 \pm 0.02$	$0.91/0.89/0.87/0.85 \pm 0.03$
$r_{Vs} (\mu\text{m}); \sigma_s$	$0.14 + 0.013\tau(440) \pm 0.01$; 0.40 ± 0.04	$0.14 + 0.01\tau(440) \pm 0.01$; 0.47 ± 0.03
$C_{VF} (\mu\text{m}^3/\mu\text{m}^2)$	$3.27 + 0.58\tau(440) \pm 0.45$; 0.79 ± 0.06	$3.27 + 0.51\tau(440) \pm 0.39$; 0.79 ± 0.04
$C_{Vs} (\mu\text{m}^3/\mu\text{m}^2)$	$0.12 \tau(440) \pm 0.05$	$0.1 \tau(440) \pm 0.06$
	$0.05 \tau(440) \pm 0.02$	$0.04 + 0.03 \tau(440) \pm 0.03$
	Bahrain–Persian Gulf (1998–2000)	Solar-Vil.–Saudi Arabia (1998–2000)
Desert dust and oceanic		
Number of measurements (total)	1800	1500
Number of measurements (for ω_0, n, k)	100	250
Range of optical thickness; $\langle\tau\rangle$	$0.1 \leq \tau(1020) \leq 1.2$; $\langle\tau(1020)\rangle = 0.22$	$0.1 \leq \tau(1020) \leq 1.5$; $\langle\tau(1020)\rangle = 0.17$
Range of Ångström parameter (g) (440/670/870/1020)	$0 \leq \alpha \leq 1.6$	$0.1 \leq \alpha \leq 0.9$
n	$0.68/0.66/0.66/0.66 \pm 0.04$	$0.69/0.66/0.65/0.65 \pm 0.04$
$k(440/670/870/1020)$	1.55 ± 0.03	1.56 ± 0.03
$\omega_0(440/670/870/1020)$	$0.0025/0.0014/0.001/0.001 \pm 0.001$	$0.0029/0.0013/0.001/0.001 \pm 0.001$
$r_{VF} (\mu\text{m}); \sigma_r$	$0.92/0.95/0.96/0.97 \pm 0.03$	$0.92/0.96/0.97/0.97 \pm 0.02$
$r_{Vs} (\mu\text{m}); \sigma_s$	0.15 ± 0.04 ; 0.42 ± 0.04	0.12 ± 0.05 ; 0.40 ± 0.05
$C_{VF} (\mu\text{m}^3/\mu\text{m}^2)$	2.54 ± 0.04 ; 0.61 ± 0.02	2.32 ± 0.03 ; 0.60 ± 0.03
$C_{Vs} (\mu\text{m}^3/\mu\text{m}^2)$	$0.02 + 0.1 \tau(1020) \pm 0.05$	$0.02 + 0.02 \tau(1020) \pm 0.03$
	$-0.02 + 0.92 \tau(1020) \pm 0.04$	$-0.02 + 0.98 \tau(1020) \pm 0.04$

2. LIDAR instruments

Lidar stands for "light detection and ranging" and is a radar-related ("radiowave detection and ranging") method to remotely measure atmospheric parameters. Lidar systems send out laser pulses and detect the backscattered radiation. From the signals' time delay and the speed of light, the distance from the backscatter location can be determined. Clouds and dust particles in air (so-called aerosols) scatter laser radiation very strongly. Therefore, a simple application of lidar is the highly resolved detection and distance determination of clouds and aerosol layers.

2.1. PRINCIPLE OF LIDAR MEASUREMENT

A pulsed laser beam is sent into the atmosphere, hits air molecules and other particles, and is scattered by them. The scattered light is sent into various directions and only a small part is reflected back towards its origin. The backscattered light is then collected by telescopes and conducted into a detection unit. There, after passing through filters, the signal is received by a detector (a photo multiplier tube or a photo diode), converted into electronic signals, and recorded with temporal resolution.

From the time delay, the distance R of the scattering volume can be determined and is expressed as $R = tc/2$ with c the speed of light, t is the time between emission of the laser pulse and reception of the backscattered radiation. The maximum range resolution ΔR depends on the length of the laser pulse (~ 10 ns), the time constant of the detecting electronics (50 to 200 ns), and the reaction time of the interaction of laser light with particles (negligible). Micro-pulse lidar uses low pulse energy ($\sim 6-8 \mu\text{J}$) at high frequency (2500Hz) which is well below the $25 \mu\text{J}$ ANSI eye-safety threshold, but requires pulse summation to increase signal to noise ratio (up to 1 minute).

Lidar equation

The power P_L of the backscattered light is given by the so-called lidar equation: $P_L(z, \lambda) = KG(z)\beta(z)T(z)$

The received power depends on 4 terms:

1. C system constant:
2. Geometry factor $G(z)$ contains the overlap function of the laser beam with the receiver field of view $O(z^2)$

$$P_L(z, \lambda) = C_L \frac{\beta_R(z, \lambda) + \beta_A(z, \lambda)}{z^2} \exp\left[-2 \int_0^z [\varepsilon_R(z', \lambda) + \varepsilon_A(z', \lambda)] dz'\right]$$

Where $P_L(z, \lambda)$ is the received lidar signal at range z [m] and wavelength λ [m], C is the system constant, $\beta(z, \lambda)$ is the backscatter coefficient [m^{-1}]

sr^{-1}] and $\varepsilon(z, \lambda)$ is the extinction coefficient [m^{-1}], the R subscript denotes Rayleigh quantity and the A subscript denotes aerosol quantity. Knowing air density profile $\beta_R(z, \lambda)$ and $\beta_A(z, \lambda)$ can be calculated at any given range z , and wavelength λ . Two unknowns $\beta_A(z, \lambda)$ and $\varepsilon_A(z, \lambda)$ remain for one equation.

The backscatter coefficient is related to the extinction by $\beta(z) = S(z)\varepsilon(z)$, where $S(z)$ is the backscatter-extinction ratio [sr^{-1}]. By assuming S constant with altitude, the range corrected lidar signal is given by

$$P_r(z) = z^2 P_L(z) = C_L [\beta_A(z) + \beta_R(z)] \times \exp\left[-\frac{2}{S_R} \int_0^z \beta_R(z') dz'\right] \times \exp\left[-\frac{2}{S_A} \int_0^z \beta_A(z') dz'\right]$$

and it can be solved for $\beta_A(z)$. The range corrected lidar profile P_r divided by the lidar constant C is referred as Attenuated Backscatter Signal (ABS) profile. The solution of the lidar equation depends on the type of instrument.

Solution of LIDAR equation

a. BACKSCATTER LIDAR



The $\beta_A(z)$ solution of the lidar data is given by:

$$\beta_A(x-1) = \frac{P_r(x-1) \times \Psi(x-1, x)}{\frac{P_r(x)}{\beta_A(x) + \beta_R(x)} + \frac{1}{S_A} [P_r(x) + P_r(x-1)\Psi(x-1, x)] \Delta z} - \beta_R(x-1)$$

$$\Psi(x-1, x) = \exp\left[\left(\frac{1}{S_A} - \frac{1}{S_R}\right) \times (\beta_R(x-1) + \beta_R(x)) \Delta z\right]$$

Where x is the altitude bin one step above $x-1$, Δz is the lidar range interval. The values $\beta_A(z)$ are evaluated iteratively:

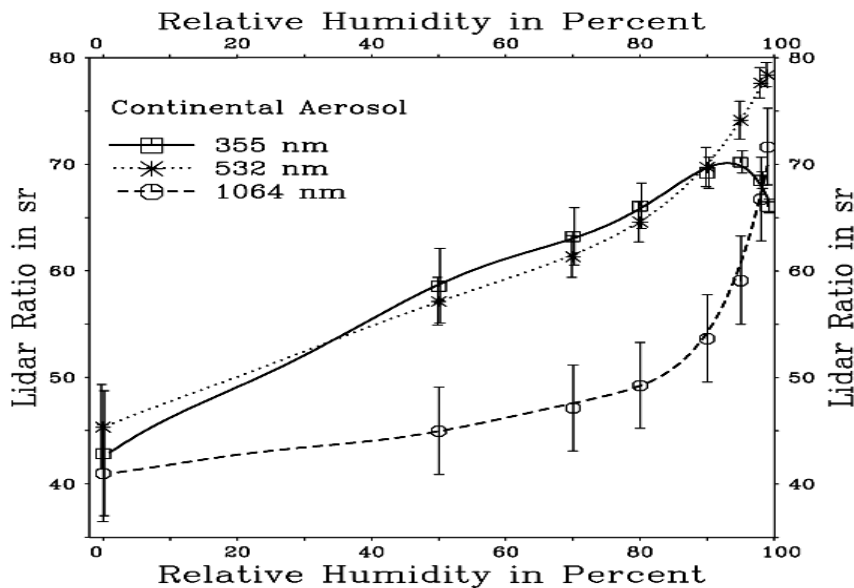
- i. Set an initial value of $S_A=1$
- ii. Set a boundary condition at high altitude z_m such that $\beta_A(x_m - 1) = 0$
- iii. Calculate successively $\beta_A(x_m - 1)$, $\beta_A(x_m - 2)$, ..., $\beta_A(z = 0)$

- iv. Calculate $S_A = \frac{0}{\tau_A}$ with the value τ_A measured independently (e.g. sunphotometer).

- v. If the difference between the first guess of S_A and its last value is greater than a threshold values (e.g. 0.5) then restart the calculation at iii with the new value of SA
- vi. Do a final calculation of β_A , S_A , $\varepsilon_A = \frac{\beta_A}{S_A}$, and τ_A profile from

lidar altitude to z_m

For submicron particles, S_A value is about 30 sr, but higher values for hygroscopic particles at increasing RH.



b. SCANNING BACKSCATTER LIDAR

c. RAMAN LIDAR

Raman lidar systems detect, in addition to backscattering at the laser wavelength (elastic backscattering), also signals at different wavelengths. These signals emerge from scattering by molecules, which absorb a part of the photon's energy or add an amount of energy to the photon's energy (inelastic scattering).

By inelastic scattering, these molecules change their vibrational and/or rotational state (Raman process). The backscattered light experiences a frequency shift caused by its change of energy.

Raman backscattering from gases of known number concentration (oxygen, nitrogen) serves as an atmospheric reference. Therefore, Raman nitrogen/oxygen signals can be used to retrieve aerosol extinction coefficients and to determine ozone concentrations using the so-called Raman DIAL technique.

Example of Raman Lidar:

Emission @ 532 nm

Detection @ 532 nm (elastic backscatter)

Detection @ 607 nm (N₂ Raman backscatter)

Two lidar equations:

$$P(z, \lambda_0) = C_L \frac{\beta_R(z, \lambda_0) + \beta_A(z, \lambda_0)}{z^2} \exp \left[-2 \int_0^z [\varepsilon_R(z', \lambda_0) + \varepsilon_A(z', \lambda_0)] dz' \right]$$

$$P(z, \lambda_{Raman}) = C_{Raman} \frac{\beta_{Raman}(z, \lambda_0)}{z^2} \exp \left[-2 \int_0^z [\varepsilon_R(z', \lambda) + \varepsilon_A(z', \lambda) + \varepsilon_R(z', \lambda_{Raman}) + \varepsilon_A(z', \lambda_{Raman})] dz' \right]$$

$$\varepsilon_R(\lambda_{Raman}) = \varepsilon_R(\lambda_0) \left(\frac{\lambda_{Raman}}{\lambda_0} \right)^{-\alpha} \text{ where } \alpha \text{ is the Angstrom exponent}$$

ADVANTAGE:

With a Raman Lidar, the lidar ratio S is no more an input parameter but a result.

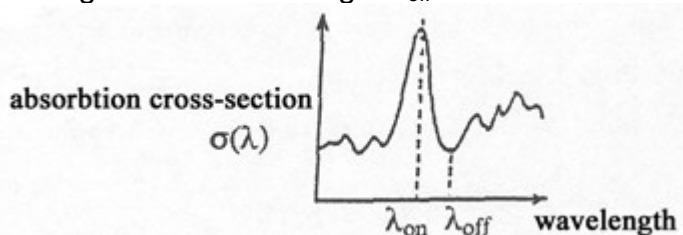
DRAWBACKS:

The Raman scattering cross sections are several orders of magnitude smaller than those for elastic scattering. Therefore, Raman lidars work with high laser pulse energy, relatively large telescopes, and efficient detectors on the basis of single-photon detection.

d. DIFFERENTIAL ABSORPTION LIDAR

DIAL allows the determination of gas concentrations, especially of water vapor, with very high spatial and temporal resolution.

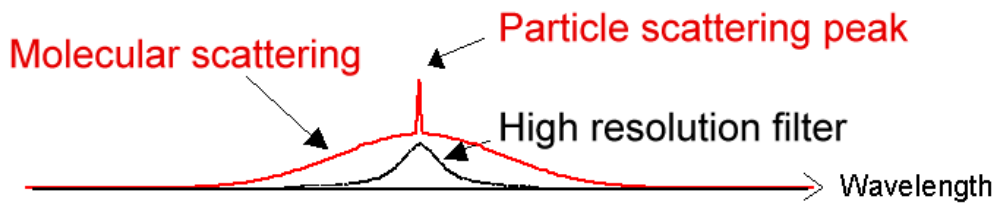
Two laser pulses with wavelengths λ_{on} and λ_{off} are emitted quasi-simultaneously. Light at the wavelength λ_{on} is absorbed by the species of interest more strongly than light at the wavelength λ_{off} .



Assuming that all other backscatter and extinction parameters in the atmosphere are the same for both wavelengths, we can determine the differential absorption coefficient in the volume of length $\Delta R = R_2 - R_1$ by comparing the signal ratios P_{on}/P_{off} from the distances R_2 and R_1 . If the differential absorption cross section of the species of interest for the two wavelengths is known, the number concentration of the gas atoms or molecules can directly be deduced.

e. HIGH SPECTRAL RESOLUTION LIDAR

Lidar with high spectral resolution filter can measure separately the return signal from molecules and aerosol particles



Two lidar equations:

$$P_R(z) = C_{LR} \frac{\beta_R(z)}{z^2} \exp \left[-2 \int_0^z [\varepsilon_R(z') + \varepsilon_A(z')] dz' \right]$$

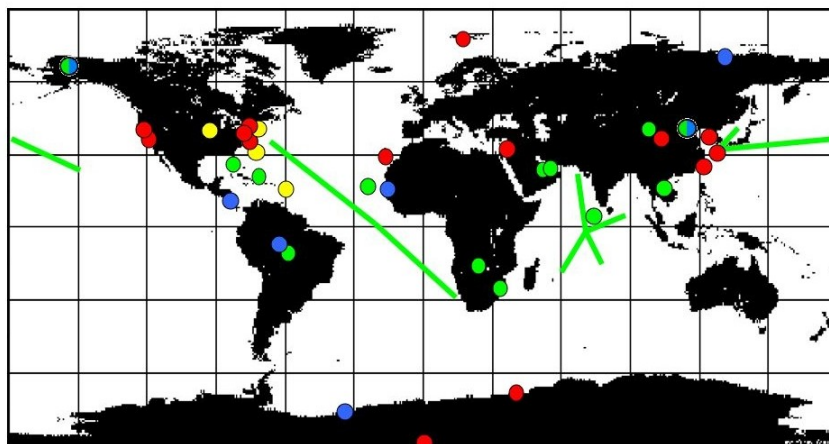
$$P_A(z) = C_{LA} \frac{\beta_A(z)}{z^2} \exp \left[-2 \int_0^z [\varepsilon_R(z') + \varepsilon_A(z')] dz' \right]$$

ADVANTAGE: The lidar ratio is a result.

DISADVANTAGE: Two calibration constants required.

2.2. NETWORK OF LIDAR INSTRUMENTS

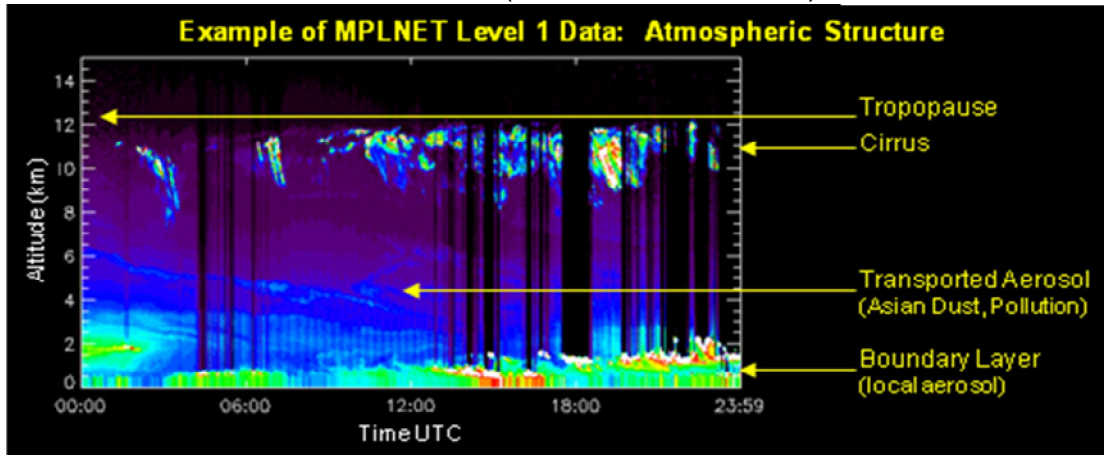
- a) **MPLNET** <http://mplnet.gsfc.nasa.gov/data.html>
- A federated network of micro pulse lidar sites around the world, coordinated and lead from Goddard Space Flight Center
 - Co-location with related networks, including NASA AERONET
 - Local, regional, and global scale contributions to atmospheric research



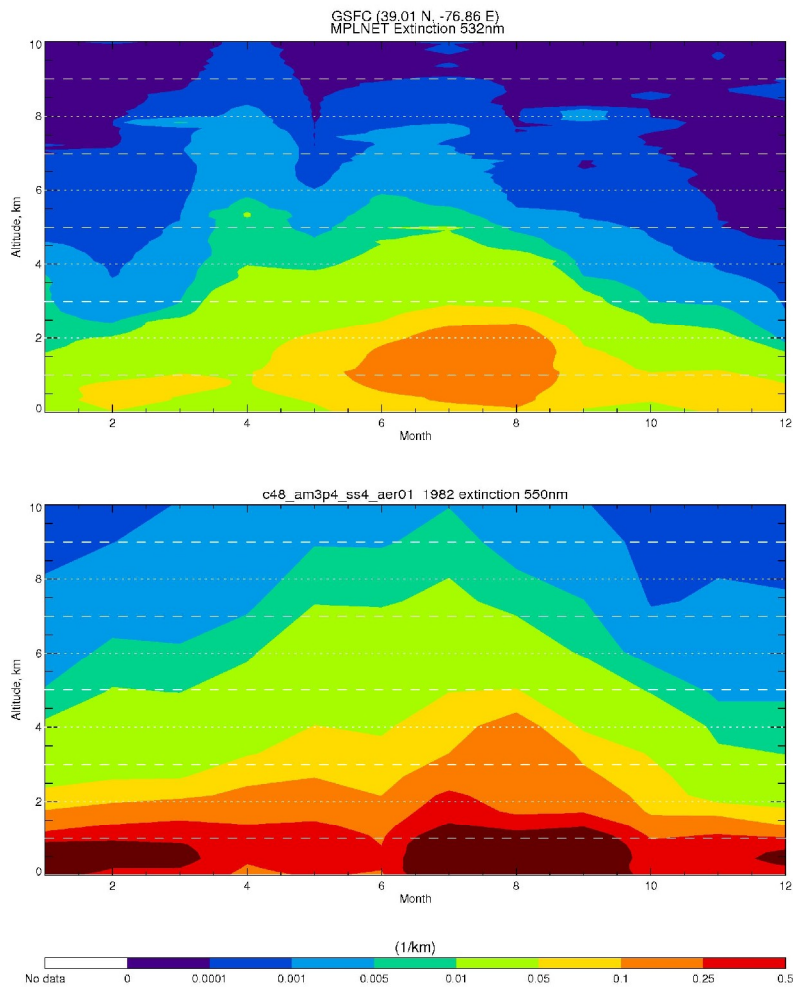
- | | |
|-------------------|--|
| ● active sites | ● former campaign, permanent site planned |
| ● field campaigns | ● former campaign, permanent site proposed |
| ● planned sites | |
| ● proposed sites | |
- most sites co-located with AERONET
- * line denotes research cruise

APPLICATION:

- (1) TIME EVOLUTION OF A DUST PLUME OVER BOUNDARY LAYER POLLUTION (1 PROFILE/MINUTE)

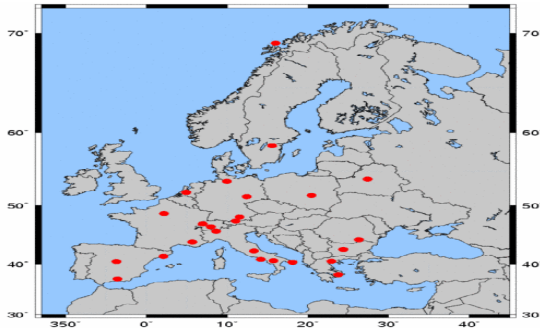


- (2) SEASONAL VARIATION OF EXTINCTION PROFILE OVER GREENBELT (MD) (MONTHLY MEAN OVER 3 YEARS OF DATA) AND COMPARISON WITH MODEL RESULTS

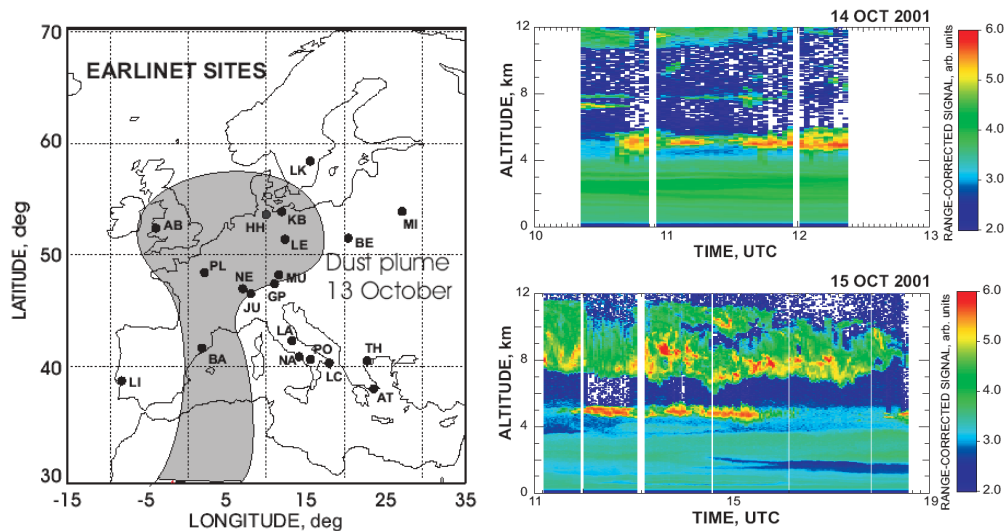


b) **EARLINET** <http://www.earlinetasos.org/>

EARLINET is a joint project of presently more than 20 European lidar stations. Each lidar group performs observations on a routine base three times a week on preselected days and times since May 2000.



Example of application: Case study of a Sahara dust storm over Europe (<http://www.gfdl.noaa.gov/reference/bibliography/2003/ansmann0301.pdf>)



c) **ASIANET** <http://www-lidar.nies.go.jp/>